Investigating the acceleration efficiency of VLF and ULF waves on different electron populations in the outer radiation belt through multi-point observations and modeling

Afroditi Nasi, Christos Katsavrias, Sigiava Aminalragia-Giamini, Nour Dahmen, Antoine Brunet, Constantinos Papadimitriou, Ingmar Sandberg, Sébastien Bourdarie, Viviane Pierrard, Edith Botek, et al.

Investigating the acceleration efficiency of VLF and ULF waves on different electron populations in the outer radiation belt through multi-point observations and modeling

Afroditi Nasi, et al.
NKUA, Greece, afnasi@phys.uoa.gr

Sharing is encouraged

Scan the QR for abstract info & for the full list of authors and affiliations

1. INTRODUCTION

- During the second half of 2019, the Earth's magnetosphere was impacted by a sequence of isolated Corotating Interaction Regions (CIRs) during four consecutive solar rotations.
- The 3rd CIR group arrived during August-September 2019 and resulted in significant multi-MeV electron enhancements, up to 9.9 MeV.
- In order to assess the relative contribution of radial diffusion and gyro-resonant acceleration, focusing on this 3rd CIR group, we study the electron Phase Space Density (PSD) in two ways, by:
  - Producing PSD radial profiles using data from several satellites.
  - Producing PSD temporal profiles using several numerical simulation models.
- Additionally, we inspect the dependence of the PSD profiles on the values of the first and second adiabatic invariants (μ,K).

2. EVENT DESCRIPTION & PROPERTIES

Figure 1. Solar wind & geomagnetic parameters

Solar wind parameters (Vsw [km/s], Psw [nPa] (OMNIWeb)) and geomagnetic indices (SYM-H [nT] (OMNIWeb), SML [nT] (SuperMAG)) during the period of interest (1/7-15/10/2019), including all the CIR groups, indicated by magenta lines. The four CIR groups exhibit similar Vsw and Psw structure and result in weak storm activity, with only the 3rd CIR group exhibiting intense substorm activity.

Figure 2. VLF wave activity

MLT-averaged amplitude [nT] of Very Low Frequency (VLF) lower-band whistler-mode chorus waves, calculated following Li et al., 2013, using POES&MetOp/SEM-2 data. Again, only the 3rd CIR group resulted in intense and prolonged VLF wave activity, following the substorm activity. (We also note that this is the case for the ULF Pc4-5 wave power spectral density as well, as calculated following Katsavrias et al., 2022 and shown in Nasi et al., 2022).

Figure 3. Electron flux intensity

The logarithm of omni-directional electron flux intensity [(MeV cm^2 sr s)$^{-1}$] for ultra-relativistic electrons of E = 4.2, 7.7, and 9.9 MeV (RBSP-A/MegEIS&REPT, cleaned and slightly rescaled using Arase/XEP as a reference, following Sandberg et al., 2021). We notice that only the 3rd CIR group results in intense, discreet and prolonged energization of all shown electron populations, even up to 9.9 MeV.

3. ELECTRON PHASE SPACE DENSITY (PSD)

3.1. PSD OBSERVATIONS

Figure 4. Electron PSD radial profiles

Radial profiles of the PSD, covering only the first part of the 3rd CIR group (28/8-4/9/2019). The PSD is calculated following Nasi et al., 2020, using Arase/HEP, Arase/MGF, RBSP-A/MagEIS&REPT, RBSP-A/FXG, all combined for L*<5.8, and THEMIS/SST, THEMIS/FGM for L*>5.8. The PSD radial profiles are produced for three values of the first and second adiabatic invariants: μ = 100, 1000 and 5000 MeV/G, and K = 0.03, 0.09 and 0.15 $G^{1/2}R_E$. (More details in Nasi et al., 2022).

Conclusions:

Panel (B):
K = 0.03 $G^{1/2}R_E$ (near-equatorial mirroring), μ = 1000 MeV/G (relativistic)
Rising peaks at L* = 4.5-5 indicate local acceleration via VLF chorus waves.

Panel (C):
K = 0.03 $G^{1/2}R_E$ (near-equatorial mirroring), μ = 5000 MeV/G (ultra-relativistic)
Fast gradients (but with lack of sufficient data on high L*)
probably indicate inward radial diffusion driven by ULF Pc4-5 waves.

Panels (D)-(I):
Higher-K PSD profile evolution indicates local acceleration by chorus waves.

This part of the work, included in this white box, has been published in **Nasi et al., 2022**

At L* = 4.5, covering all K values:	
μ = 100 MeV/G	E = 0.2 – 0.5 MeV
μ = 1000 MeV/G	E = 1 – 2 MeV
μ = 5000 MeV/G	E = 2.8 – 5 MeV

Figure 1. Solar wind & geomagnetic parameters

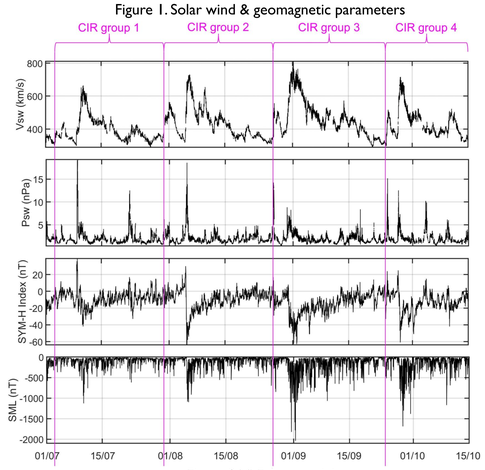

Figure 2. VLF wave activity

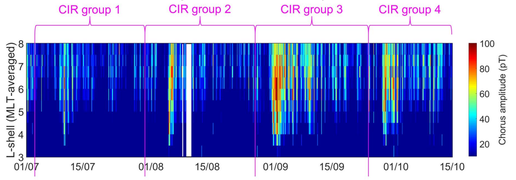

Figure 3. Electron flux intensity

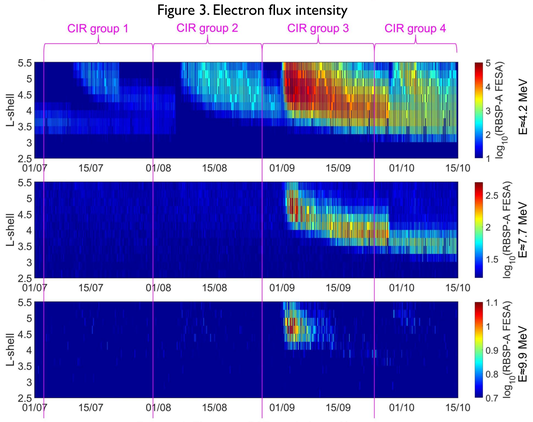

Figure 4. Electron PSD radial profiles

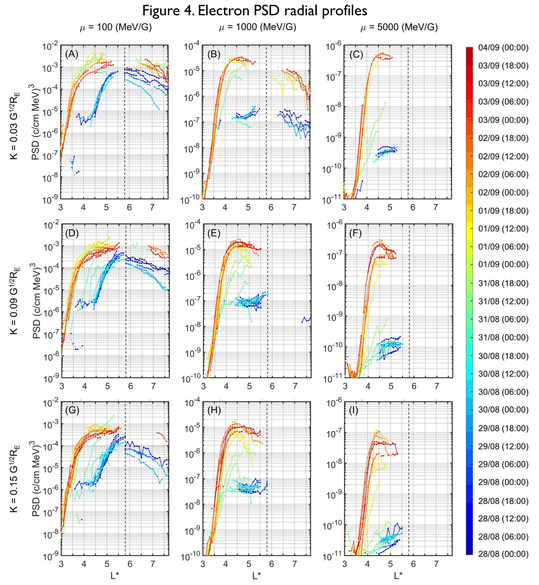

3.2. PSD SIMULATIONS

Figure 5. Electron PSD temporal profiles

Using the relevant models mentioned in Section 3.3., we produced temporal profiles of the electron PSD, focusing on the 3rd CIR group (28/8-15/9/2019).

The format of the shown results, for each μ and K value, is as follows:

PSD_{OBS}	Observed PSD, calculated with RBSP, Arase, THEMIS data (as in 3.1.)
PSD_{ALL}	Simulated PSD including all mechanisms (rad. dif. & loc. acc.)
PSD_{DLL}	Simulated PSD including radial diffusion only
PSD_{ALL} / PSD_{OBS}	The ratio of the all mechanism simulation over the observations
PSD_{DLL} / PSD_{OBS}	The ratio of radial diffusion simulation over the observations

L* T

Figure 5. Electron PSD temporal profiles

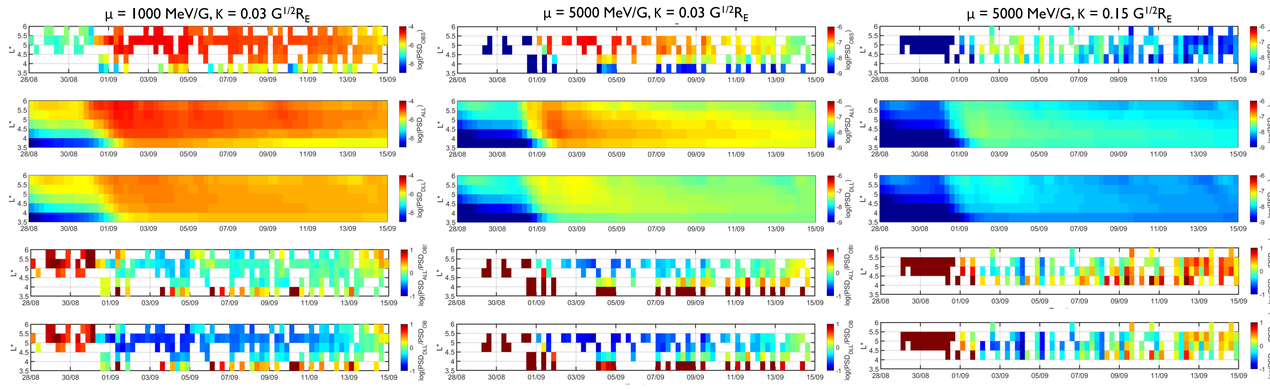

The PSD_{ALL} describes the PSD_{OBS} more accurately, with the ratio of PSD_{ALL}/PSD_{OBS} being generally larger than the PSD_{DLL}/PSD_{OBS} ratio, and closer to 0, indicating that local acceleration via chorus waves is dominant for the acceleration of the μ = 1000 MeV/G electrons, as also indicated by the radial profiles shown in Section 3.1.

The PSD_{DLL} seems to overly underestimate the PSD_{OBS}. However, this is also true considering the PSD_{ALL}, which also seems unable to fully reproduce the PSD_{OBS}. In the same time, the ratios seem virtually similar, making the μ = 5000 MeV/G and K = 0.03 $G^{1/2}R_E$ case inconclusive about the relative role of the two acceleration mechanisms.

On the other hand, in the case of μ = 5000 MeV/G and K = 0.15 $G^{1/2}R_E$, corresponding to more off-equatorial mirroring populations, the PSD_{ALL} describes the PSD_{OBS} more accurately, again with the PSD_{ALL}/PSD_{OBS} ratio being closer to 0, indicating that local acceleration via chorus waves again plays an important part.

3.3. SIMULATION INFO

In order to reproduce the observations, we performed numerical simulations of the radiation belt environment, which we plotted as PSD temporal profiles, again focusing on the 3rd CIR group. This was done in the scope of the EU-H2020 SafeSpace Research Programme.

We utilized and combined several relevant models:
- EMERALD (NKUA)
- GEO model (NKUA)
- Salammbô (ONERA)
- VLF model (IAP)
- Plasmaspheric model (BIRA-IASB)
- FARWEST (ONERA)

We reproduced two scenarios:
- One including all mechanisms (radial diffusion & local acceleration)
- One including radial diffusion only

safespace-h2020.eu

4. DISCUSSION & CONCLUSIONS

- In all shown cases, the PSD_{DLL} seems to underestimate the PSD values.
- The μ = **1000** MeV/G, K = **0.03** $G^{1/2}R_E$ electrons is the only shown case where the simulation including all mechanisms best describes the observations of the PSD. Both their temporal profiles and ratios indicate that **local acceleration** via VLF chorus waves seems to be the **dominant** mechanism for their acceleration, as also indicated by the PSD radial profiles.
- The μ = **5000** MeV/G, K = **0.03** $G^{1/2}R_E$ electron population proved **inconclusive** on the relative role of the acceleration mechanisms, contrary to the indications of the corresponding radial profiles. Even the simulation including all mechanisms is unable to reproduce the observations.
- However, moving on to the μ = **5000** MeV/G, K = **0.15** $G^{1/2}R_E$ electron population, **local acceleration** via chorus waves again becomes **prominent**, event though both simulation cases do not reproduce the observations closely.
- Generally, plots for higher K values (K = 0.09 and 0.15 $G^{1/2}R_E$, for all μ values, not shown in this poster) indicate that local acceleration becomes more important moving to off equatorial mirroring populations, even though this could be due to the fact that radial diffusion in more important for near-equatorial mirroring populations.
- The plots of the simulated PSD, and especially the plots of the ratios, could prove unreliable as the PSD used in the radial profiles has been calculated with the TS04 model, while the PSD used in the temporal profiles has been calculated with the OPQ model.

5. FUTURE WORK

- Compare the observed PSD calculated with OPQ (used in the simulations) vs the PSD calculated with TS04 (used for the radial profiles).
- Produce radial profiles using the simulated PSD.
- Investigate possible timelags.
- Incorporate errors in the PSD calculation.

6. REFERENCES

- **Katsavrias et al. (2022)**. The "SafeSpace" database of ULF power spectral density and radial diffusion coefficients: dependencies and application to simulations. Annales Geophysicae, 40, 379–393, 2022. doi: 10.5194/angeo-40-379-2022
- **Li et al. (2013)**. Constructing the global distribution of chorus wave intensity using measurements of electrons by the POES satellites and waves by the Van Allen Probes. Geophys. Res. Lett. 40, 4526–4532. doi: 10.1002/grl.50920
- **Nasi et al., (2020)**. Interplay of source/seed electrons and wave-particle interactions in producing relativistic electron PSD enhancements in the outer Van Allen belt. J. Atmos. Solar-Terrestrial Phys. 210, 105405. doi: 10.1016/j.jastp.2020.105405
- **Nasi et al. (2022)**. An event of extreme relativistic and ultra-relativistic electron enhancements following the arrival of consecutive corotating interaction regions: Coordinated observations by Van Allen Probes, Arase, THEMIS and Galileo satellites. Front. Astron. Space Sci. 9:949788. doi: 10.3389/fspas.2022.949788
- **Sandberg et al. (2021)**. Harmonization of RBSP and Arase energetic electron measurements utilizing ESA radiation monitor data. Space weather.,19. doi: 10.1029/2020SW002692

EGU This presentation participates in OSPP Outstanding Student & PhD candidate Presentation contest

Scan the QR for a 10 min recorded presentation of this work on YouTube